

Boosting Consistency in Dual Training for Long-Tailed Semi-Supervised Learning

Kai Gan, Tong Wei, and Min-Ling Zhang, *Senior Member, IEEE*

Abstract—While long-tailed semi-supervised learning (LTSSL) has received tremendous attention in many real-world classification problems, existing LTSSL algorithms typically assume that the class distributions of labeled and unlabeled data are almost identical. Those LTSSL algorithms built upon the assumption can severely suffer when the class distributions of labeled and unlabeled data are mismatched since they utilize biased pseudo-labels from the model. To alleviate this problem, we propose a new simple method that can effectively utilize unlabeled data from unknown class distributions through **Boosting c**onsistency in **du**Al **T**raining (**BOAT**). Specifically, we construct the standard and balanced branch to ensure the performance of the head and tail classes, respectively. Throughout the training process, the two branches incrementally converge and interact with each other, eventually resulting in commendable performance across all classes. Despite its simplicity, we show that BOAT achieves state-of-the-art performance on a variety of standard LTSSL benchmarks, e.g., an averaged 2.7% absolute increase in test accuracy against existing algorithms when the class distributions of labeled and unlabeled data are mismatched. Even when the class distributions are identical, BOAT consistently outperforms many sophisticated LTSSL algorithms. We carry out extensive ablation studies to tease apart the factors that are the most important to the success of BOAT. The source code is available at <https://github.com/Gank0078/BOAT>.

Index Terms—Semi-Supervised Learning, Long-tailed learning, Consistency Regularizer, Distribution Estimation.



1 INTRODUCTION

SEMI-SUPERVISED learning (SSL) is an effective way to use unlabeled data to improve the generalization of deep neural networks (DNNs) [1], [2], [3] when only a limited amount of labeled data is accessible [4], [5], [6], [7]. The core idea of most SSL algorithms is to generate pseudo-labels for unlabeled data and select confident ones to train models. Recent progress on SSL has revealed promising performance in various tasks, such as image recognition [7] and text categorization [8], [9]. Popular SSL methods [10], [11], [12] employ a confidence threshold to select reliable pseudo-labels, thereby enhancing the model’s generalization capability. However, most existing SSL algorithms assume that the datasets are class-balanced, i.e., each class is associated with an equivalent number of samples in both labeled and unlabeled datasets. In contrast, class distributions in many real-world tasks are long-tailed [13], [14], [15], [16], [17]. It is well known that classifiers trained on long-tailed datasets tend to be biased towards majority classes, leading to low test accuracy on minority classes [18], [19], [20].

To improve the performance, many long-tailed semi-supervised learning (LTSSL) algorithms have been proposed to generate unbiased pseudo-labels. They pursue class-balanced classifiers using techniques including re-sampling [21], re-weighting [22], label smoothing [23], and pseudo-label alignment [24], [25], [26]. These algorithms have shown strong generalization for the minority class by assuming

that the class distributions of labeled and unlabeled data are almost identical. However, this assumption is frequently violated in real-world applications, for instance, if the labeled and unlabeled data are collected from different tasks. Unlabeled data may have a large class distribution deviation from labeled data, and the use of an erroneous assumption can severely deteriorate performance [22], [27]. Recently, some LTSSL methods [27], [28] attempt to address this class distribution shift between labeled and unlabeled data. However, these methods consider specific distributions of unlabeled data, rendering them ineffective in handling arbitrary unlabeled data distributions.

This paper studies the underexplored yet practical LTSSL problem, i.e., learning from unlabeled data of unknown class distributions. In particular, we start with three representative types of class distributions of unlabeled data following [27], i.e., *consistent*, *uniform*, and *reversed*, as illustrated in Fig. 1. It is noteworthy that this paper focuses on any arbitrary unlabeled data distribution that is not limited to three representative distributions, and experiments on more unlabeled data distributions are presented in Sec. 4.4. We then propose a new simple algorithm BOAT, which is built on one of the most popular SSL algorithms, FixMatch [7], to boost the consistency in dual training for LTSSL tasks.

In realistic LTSSL settings, if we directly apply SSL methods to the imbalanced labeled and unlabeled data, the model’s predictions will significantly favor the head classes. However, recent LTSSL methods [28], [29] that introduce balanced modules can result in model bias towards the tail class, thus hurt the head class performance. Therefore, we design a dual-branch architecture to ensure the performance of both head and tail classes separately. The first branch, referred to as the **standard branch**, aims to maintain the performance of head classes. The standard branch does

- Kai Gan, Tong Wei, and Min-Ling Zhang are with the School of Computer Science and Engineering, Southeast University, Nanjing 210096, China, and the Key Laboratory of Computer Network and Information Integration (Southeast University), Ministry of Education, China. E-mail: {gank,wei,tzhangml}@seu.edu.cn.

Corresponding author: Tong Wei.

not implement any transformation on the pseudo-labels, ensuring it does not overly shift towards the tail classes like recent LTSSL methods. The other branch, termed the **balanced branch**, attempts to maintain the performance on tail classes by adjusting the model’s predictions on the unlabeled data. However, even if both branches ideally achieve their intended objectives, integrating the two branches during inference remains a significant challenge, which has been extensively discussed in previous studies [15], [16], [30] and a satisfactory solution to this problem remains elusive. Therefore, in this paper, we do not combine the predictions of the two branches as the final inference result. Instead, we facilitate interactions between the branches during the training, enabling both to achieve superior performance on both head and tail classes progressively.

Specifically, we avoid directly applying any balancing strategy to the pseudo-labels derived from unlabeled data for the standard branch, allowing it to achieve strong performance on head classes [30]. In addition, for the balanced branch, we apply a popular rebalancing strategy in long-tailed learning, i.e., logit adjustment [31], to alleviate the model’s excessive focus on head classes, thus enabling it to sustain strong performance on tail classes. Regarding the interaction between the two branches, this is primarily manifested in two aspects: i) the output of the standard branch for unlabeled samples undergo rebalancing adjustment and then serve as the targets for the balanced branch, whereas ii) the distribution predicted by the balanced branch for unlabeled data will be used to align the labeled data in the standard branch. As training progresses, it is observed that the predictive tendencies of the two branches gradually converge. Furthermore, both branches, especially the balanced branch, can realize significant pseudo-label accuracy on unlabeled datasets and achieve outstanding performance on both head and tail classes. During the inference phase, we significantly improved the model’s performance on the balanced test set using post-hoc enhancement, which further balances the predictions.

We demonstrate the effectiveness of the proposed approach under various realistic LTSSL scenarios by varying the class distributions of unlabeled data. Despite its simplicity, the proposed algorithm improves recent LTSSL algorithms in all test cases, e.g., our method improves DARP [25], DASO [27], ACR [28] with up to **11.2%**, **8.1%**, and **2.4%** absolute increase in test accuracy, respectively. In addition to three types of representative class distributions, i.e., *consistent*, *uniform*, and *reversed*, we also test BOAT under many other class distributions in Sec. 4.4. As expected, our method significantly improves performance when class distributions are mismatched between labeled and unlabeled data.

2 RELATED WORK

Long-tailed learning. Research on long-tailed learning has attracted increasing attention recently, which is a challenging and practical task. The main directions to improve the performance include: 1) data manipulation [13], [32], 2) representation learning [17], [33], and model output adjustment [31], [34]. Data manipulation is often encompassed by the design of resampling strategies and the implementation of data augmentation techniques. Numerous studies

have demonstrated performance enhancements through the adoption of a two-stage training paradigm, where the initial stage is dedicated to learning data representations, followed by a subsequent stage that focuses on classifier training [32]. The adjustment of the model’s output can be executed during the training phase through the optimization of unbiased loss functions, or post-hoc adjustments can be implemented. In this paper, considering the firm statistical grounding and commendable empirical performance of the logit adjustment [31], BOAT predominantly employs this technique to mitigate the effects of the long-tailed distribution.

Semi-supervised learning. A popular class of Semi-supervised learning (SSL) algorithms use unlabeled data to improve the performance via learning to predict the pseudo-labels produced by the model, which can be viewed as a self-training process [4], [5], [6], [35]. Recent SSL algorithms [7], [35] combine pseudo labeling and consistency regularization, which encourages similar predictions between two different views of an image, to improve the robustness of DNNs. As a representative approach, FixMatch [7] achieves significantly more superb performance than many other SSL algorithms in the image recognition task. Hence, the performance of the SSL algorithm is quite sensitive to the quality of pseudo-labels. To improve the quality of pseudo-labels, [10], [11], [12] employ thresholding or weighting schemes to select high-quality pseudo-labels for training. FlexMatch [10] allocates unique thresholds to individual classes, considering the varying degrees of learning difficulty and the aggregate pace of learning. FreeMatch [11] seamlessly integrates global and local threshold adjustments, complemented by a class-fairness regularization technique that promotes diversity in the model’s predictions. SoftMatch [12] effectively balances the trade-off between quantity and quality through a unified approach by sample reweighting, facilitated by a soft confidence threshold mechanism. However, most existing SSL algorithms assume balanced class distributions of labeled and unlabeled data, resulting in poor generalization of the minority class due to biased pseudo-labels. Our BOAT is built upon FixMatch, which has been frequently used as the base model for SSL tasks.

Long-tailed semi-supervised learning. Long-tailed semi-supervised learning (LTSSL) has received significant attention for its practicality in many real-world tasks. For instance, DARP [24] and CReST [25] propose eliminating biased pseudo-labels generated by the model by distribution alignment to refine pseudo-labels according to the class distribution of labeled data. ABC [21] uses an auxiliary balanced classifier trained by down-sampling majority classes to improve the generalization. CoSSL [36] designs a novel feature enhancement module for the minority class using mixup [37] to train balanced classifiers. Although these algorithms can significantly enhance performance, they assume identical class distributions of labeled and unlabeled data which is not always satisfied in real-world scenarios. DASO [27] proposes to handle this issue by employing a dynamic combination of linear and semantic pseudo-labels based on the current estimated class distribution of unlabeled data. It is noted that the accuracy of semantic pseudo-labels in DASO relies on the discrimination of learned representations. However, long-tailed class distribution negatively impacts representation learning, reducing

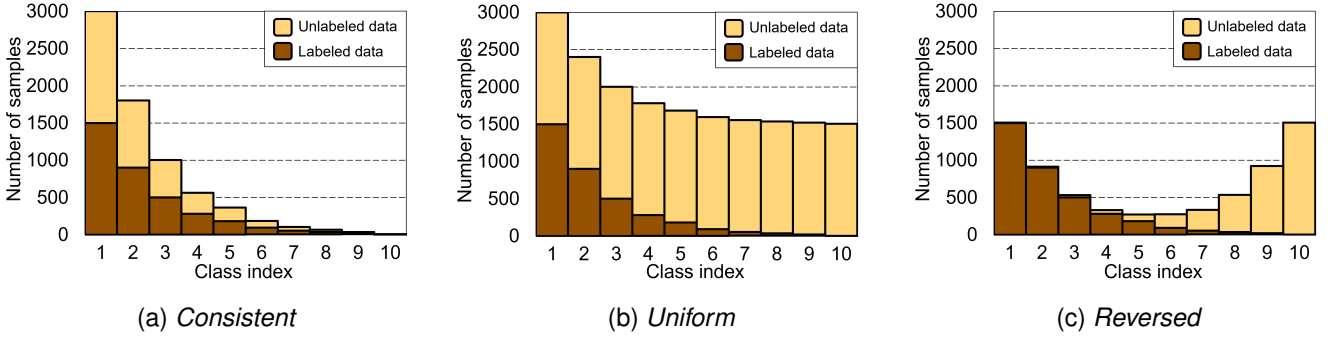


Fig. 1. 1a to 1c): Three typical types of class distribution of unlabeled data: *consistent*, *uniform*, and *reversed*.

the reliability of semantic pseudo-labels. SimPro [29], which is grounded in a probabilistic model, refines the expectation-maximization (EM) algorithm by explicitly decoupling the modeling of conditional and marginal class distributions to handle unknown unlabeled data distribution. The recent state-of-the-art method ACR [28] employs three fixed anchor distributions to dynamically tune the intensity of logit adjustment, thereby effectively addressing the challenges presented by *consistent*, *uniform*, and *reversed*. Nevertheless, ACR has been observed to perform optimally only with the three specified unlabeled data distributions due to the rigidity of the anchor distributions. When confronted with more diverse unlabeled data distributions, the efficacy of ACR is notably diminished. BOAT imposes no assumptions on unlabeled data distribution, enabling robust performance across arbitrary unlabeled data distributions. Notably, when considering *consistent*, *uniform*, and *reversed*, BOAT still significantly outperforms ACR by a considerable margin.

3 THE PROPOSED METHOD

In this section, we first introduce the preliminaries related to the LTSSL tasks and our method. Next, we present the BOAT to handle the unknown class distribution of unlabeled data with two processes and post-hoc enhancement to further improve the performance during the inference. Finally, we discuss the key distinctions between BOAT and ACR to highlight the superiority of BOAT.

3.1 Preliminaries

Problem setup. In LTSSL tasks, we have a labeled dataset $\mathcal{D}^l = \{(x_i^{(l)}, y_i^{(l)})\}_{i=1}^N$ of size N and an unlabeled dataset $\mathcal{D}^u = \{x_j^{(u)}\}_{j=1}^M$ of size M , where $x_i^{(l)}, x_j^{(u)} \in \mathbb{R}^d$ are d -dimensional feature for labeled and unlabeled training samples, respectively. For the i -th labeled sample, it is associated with a ground-truth label $y_i^{(l)} \in \{0, 1\}^C$ where C is the size of output label space. Let N_c denote the number of samples for class c in the labeled dataset, we have $N_1 \geq N_2 \geq \dots \geq N_C$, and the imbalance ratio of the labeled dataset is denoted by $\gamma_l = \frac{N_1}{N_C}$. Similarly, let M_c denote the numbers of unlabeled samples for class c , and its imbalance ratio is $\gamma_u = \frac{\max_c M_c}{\min_c M_c}$ because we do not require any assumptions on the class distribution of the unlabeled dataset. Instead, we mainly consider three

representative distributions in this work, i.e., *consistent*, *uniform*, and *reversed*. Specifically, i) for *consistent* setting, we have $M_1 \geq M_2 \geq \dots \geq M_C$ and $\gamma_u = \gamma_l$; ii) for *uniform* setting, we have $M_1 = M_2 = \dots = M_C$, i.e., $\gamma_u = 1$; iii) for *reversed* setting, we have $M_1 \leq M_2 \leq \dots \leq M_C$ and $\gamma_u = 1/\gamma_l$. It is noteworthy that in Sec. 4.4, we discuss more diverse distributions of unlabeled data, including *middle* and *headtail* [29]. Our goal is to train a classifier $f : \mathbb{R}^d \rightarrow [0, 1]^C$ parameterized by θ using \mathcal{D}^l and \mathcal{D}^u .

Semi-supervised learning. Many existing SSL algorithms seek to minimize a supervised classification loss on labeled data and an unsupervised regularizer on unlabeled data. Formally, the objective function is given as follows:

$$\min_{\theta \in \Theta} \underbrace{\sum_{i=1}^N \ell(f(x_i^{(l)}; \theta), y_i^{(l)})}_{\text{supervised } (\mathcal{L}^{\text{labeled}})} + \underbrace{\sum_{j=1}^M \Omega(x_j^{(u)}; \theta)}_{\text{unsupervised}}, \quad (1)$$

where ℓ denotes the cross-entropy loss, $\Omega(x_j^{(u)}; \theta)$ is a per-sample regularizer. Particularly, in FixMatch [7], Ω is realized by the per-sample consistency regularization:

$$\mathcal{L}_{\text{con}} = \sum_{j=1}^M \underbrace{M(x_j^{(u)})}_{\text{sample mask}} \underbrace{\ell(f(\mathcal{A}(x_j^{(u)})), q_j)}_{\text{consistency}}, \quad (2)$$

where q_j is the pseudo-label of $x_j^{(u)}$ predicted by f , the sample masks $M(x_j^{(u)}) := \mathbb{I}(\max(\delta(f(x_j^{(u)}))) \geq \rho)$ selects unlabeled samples whose predicted confidence is higher than a predefined threshold ρ ($\rho = 0.95$ for FixMatch). Here, $\delta(\cdot)$ is the softmax function and $\mathbb{I}(\cdot)$ is the indicator function. To generate another view for each sample, $\mathcal{A}(x_j^{(u)})$ represents the specific augmentation scheme for $x_j^{(u)}$, such as Cutout [38] and RandomAugment [39]. Incorporating the consistency regularizer improves the model’s robustness to spurious feature patterns.

Latterly, LTSSL methods have been prevalently inspired by long-tailed learning strategies, such as re-sampling [25] and logit adjustment [28], [31]. However, an excessive focus on tail classes caused by long-tailed learning strategies may lead to a degradation in the performance of head classes, while common SSL methods tend to induce a significant bias towards head classes. In realistic LTSSL tasks, we identify classes with a higher number of samples in the whole training set which includes labeled and unlabeled data as

head classes and those with fewer samples as tail classes. This definition differs from the traditional LTSSL methods, which define head and tail classes based solely on labeled data. In practice, attaining satisfactory performance for both head and tail classes simultaneously presents significant challenges. Therefore, we employ a double-branch network with a standard branch (denoted by f) and a balanced branch (denoted by \tilde{f}) to emerge the training of the standard classifier and a class-balanced classifier, which are designed to ensure the performance of head and tail classes separately during the training.

Can the double branch network handle unknown class distributions of unlabeled data? We respond to this question with two processes in our proposed method BOAT: i) the standard and balanced branch respectively ensure the model's performance on the head and tail classes, and ii) the interactions between the two branches incrementally guarantee performance for all classes as training progresses. We elaborate on these two processes in the following.

3.2 Head-Tail Dual Training

To achieve the first process, we leverage the loss from the labeled data to guide the two branches in focusing on the head and tail classes, respectively.

Specifically, for the balanced branch, we hope to skew the predictions of samples suitably towards minority classes so that we can mitigate the model's excessive bias towards head classes and improve performance on tail classes. Therefore, we optimize the balanced softmax [31], [34] on labeled data, which is an improved standard cross-entropy:

$$\mathcal{L}_{\text{b-labeled}} = - \sum_{i=1}^N \log \frac{e^{\tilde{f}_{y_i^{(l)}}(x_i^{(l)}) + \log \pi_{y_i^{(l)}}}}{\sum_{c=1}^C e^{\tilde{f}_c(x_i^{(l)}) + \log \pi_c}}, \quad (3)$$

where π_c is class prior $\mathbb{P}(y = c)$ which is approximated by the empirical frequency on the labeled samples. We can obtain more balanced predictions by minimizing Eq. (3).

For the standard branch, we expect it to predict more accurate pseudo-labels for head classes. Ideally, standard cross-entropy loss should be sufficient to obtain outstanding performance on the head classes. However, as training progresses, reliance on cross-entropy can significantly bias the model, especially when the distribution of unlabeled data diverges from the labeled data distribution, leading to a substantial number of incorrect pseudo-labels. Therefore, we choose to align the standard branch to decoupled unlabeled distribution through the accurate supervision information from labeled data:

$$\mathcal{L}_{\text{labeled}} = - \sum_{i=1}^N \log \frac{e^{f_{y_i^{(l)}}(x_i^{(l)}) + \tau_s \cdot \Delta_{y_i^{(l)}}}}{\sum_{c=1}^C e^{f_c(x_i^{(l)}) + \tau_s \cdot \Delta_c}}, \quad (4)$$

where $\Delta_c = \log \pi_c - \log \tilde{\pi}_c$ is the adjustment factor to appropriately align the distribution of labeled data to $\tilde{\pi}_c$. $\tilde{\pi}_c$ is the decoupled unlabeled distribution estimated by EMA (Exponential Moving Average) by \tilde{f} :

$$\tilde{\pi} = m\tilde{\pi} + (1 - m)\tilde{p}, \quad (5)$$

$$\tilde{p} = \frac{1}{B + \mu B} \left(\sum_{i=1}^B \tilde{p}_i + \sum_{j=1}^{\mu B} \tilde{p}_j \right), \quad (6)$$

where $m \in [0, 1)$ is the EMA coefficient, B represents the batch size for labeled data, and μ is a hyperparameter used to control the relative batch size ratio between labeled and unlabeled data. \tilde{p} is the estimated distribution by \tilde{f} considering all samples in a batch. \tilde{p}_l and \tilde{p}_u denote the prediction after softmax for labeled and unlabeled data, respectively. The adjustment based on π_c can mitigate the imbalance in labeled data, and $\tilde{\pi}_c$ helps f align more closely with the decoupled unlabeled distribution. Notably, the pseudo-label distribution is estimated by the balanced branch \tilde{f} rather than by f itself, and this is why we refer to $\tilde{\pi}_c$ as decoupled unlabeled distribution. We posit that this strategy can mitigate the conformation bias often observed in SSL tasks [40], [41]. In fact, if we align the model's inclination to the distribution estimated by f , it will gradually bias towards its own predictions, leading to an accumulation of preferences and incorrect pseudo-labels that ultimately affect accuracy. The alignment for $\tilde{\pi}_c$ can ease reliance on f and mitigate the risk of accumulating errors.

Despite Eq. (4) seems to lack deliberate attention to head classes with the alignment to $\tilde{\pi}_c$, it is worth noting that the decoupled unlabeled distribution portrays a subtle bias towards balanced distribution and more importantly, it also reflects the true distribution to a large degree, wherein predictions for head classes remain significantly more pronounced than those for tail classes. Consequently, the alignment in Eq. (4) can effectively contribute to enhancing the performance of head classes in standard branch.

3.3 Boosting Consistency in Dual Training

Through the head-tail dual training in Sec. 3.2, we have achieved a certain degree of interaction between two branches by the alignment to $\tilde{\pi}$ in Eq. (4), which reflects the influence of balanced branch on standard branch. Notably, this alignment also facilitates the interaction between labeled and unlabeled data, which contributes to unleash the model's performance potential [42], [43].

In addition, we propose applying a simple logit adjustment (a.k.a post-hoc logit adjustment [31]) to the output of the standard classifier f whose predicted distribution tends to favor the head classes. The refined logits are used to generate pseudo-labels, which will be treated as targets for the balanced branch. Specifically, the pseudo-label of the j -th unlabeled data $x_j^{(u)}$ used in the consistency regularizer in the balanced branch is generated by:

$$\tilde{q}(x_j^{(u)}) = \arg \max f(x_j^{(u)}) - \tau \cdot \log \hat{\pi}, \quad (7)$$

where $\hat{\pi}$ is the unlabeled distribution estimated by standard branch by EMA. The consistency regularizer for the balanced branch is:

$$\mathcal{L}_{\text{b-con}} = \sum_{j=1}^M \psi(x_j^{(u)}) \ell(\tilde{f}(\mathcal{A}(x_j^{(u)})), \tilde{q}_j), \quad (8)$$

where $\psi(x_j^{(u)}) = \gamma_t \cdot \eta(x_j^{(u)})$ represents the importance weight for the j -th unlabeled sample and $\eta(x_j^{(u)}) = \max(\delta(f(x_j^{(u)})) \cdot \delta(f(x_j^{(u)}) - \tau \cdot \log \hat{\pi}))$. γ_t scales the mag-

TABLE 1

Test accuracy of previous LTSSL algorithms and our proposed BOAT under consistent class distributions, i.e., $\gamma_l = \gamma_u$, on CIFAR-10-LT and CIFAR-100-LT datasets. The best results are in **bold**.

Algorithm	CIFAR-10-LT				CIFAR-100-LT			
	$\gamma = \gamma_l = \gamma_u = 100$		$\gamma = \gamma_l = \gamma_u = 150$		$\gamma = \gamma_l = \gamma_u = 10$		$\gamma = \gamma_l = \gamma_u = 20$	
	$N_1 = 500$ $M_1 = 4000$	$N_1 = 1500$ $M_1 = 3000$	$N_1 = 500$ $M_1 = 4000$	$N_1 = 1500$ $M_1 = 3000$	$N_1 = 50$ $M_1 = 400$	$N_1 = 150$ $M_1 = 300$	$N_1 = 50$ $M_1 = 400$	$N_1 = 150$ $M_1 = 300$
Supervised w/LA [31]	47.3±0.95 53.3±0.44	61.9±0.41 70.6±0.21	44.2±0.33 49.5±0.40	58.2±0.29 67.1±0.78	29.6±0.57 30.2±0.44	46.9±0.22 48.7±0.89	25.1±1.14 26.5±1.31	41.2±0.15 44.1±0.42
FixMatch [7]	67.8±1.13	77.5±1.32	62.9±0.36	72.4±1.03	45.2±0.55	56.5±0.06	40.0±0.96	50.7±0.25
w/ DARP [24]	74.5±0.78	77.8±0.63	67.2±0.32	73.6±0.73	49.4±0.20	58.1±0.44	43.4±0.87	52.2±0.66
w/ CReST+ [25]	76.3±0.86	78.1±0.42	67.5±0.45	73.7±0.34	44.5±0.94	57.4±0.18	40.1±1.28	52.1±0.21
w/ DASO [27]	76.0±0.37	79.1±0.75	70.1±1.81	75.1±0.77	49.8±0.24	49.2±0.35	43.6±0.09	52.9±0.42
w/ SimPro [29]	80.7±0.30	-	74.2±0.90	-	-	-	43.1±0.40	-
w/ ACR [28]	81.6±0.19	84.1±0.39	77.0±1.19	80.9±0.22	51.3±0.48	61.1±0.11	44.8±0.21	55.9±0.31
FixMatch w/ Ours	84.1±0.56	86.7±0.54	81.1±0.92	84.1±0.21	52.0±0.25	62.1±0.35	45.5±0.33	56.6±0.49

nitude of the sample weights to align with the confidence from f at epoch t :

$$\gamma_t = \sum_{j=1}^{\mu B} \max \delta(f_t(x_j^{(u)})) / \sum_{j=1}^{\mu B} \eta(x_j^{(u)}). \quad (9)$$

Notably, f_t represents the standard branch at epoch t , indicating that γ_t dynamically changes as the training progresses. Based on the definition of $\eta(x_j^{(u)})$, we can observe that it reflects the similarity of the standard branch outputs before and after the adjustment in Eq. (7). A significant distribution transformation during the adjustment will result in a small $\eta(x_j^{(u)})$, indicating that the adjustment induces substantial changes in the prediction for the sample, so the prediction after adjustment seems to be not reliable. Consequently, employing a small $\eta(x_j^{(u)})$ can reduce the weight of this sample, thus mitigating its negative influence on the training process. In contrast, when $\eta(x_j^{(u)})$ is relatively large, it suggests that the difference in the sample’s predicted outcomes before and after the adjustment is slight. Therefore, the sample’s prediction is believed to be reliable, and the sample should be assigned a higher weight to enhance its impact. More analysis related to the role of the samples’ weights is shown in Sec. 4.5.

The scaling of γ_t in Eq. (9) attempts to maintain the overall magnitude of the weights and the model’s confidence consistently. γ_t guarantees that initially, due to insufficient training, the weights remain relatively low. As training progresses and the model becomes increasingly confident in its predictions, the corresponding weights should be concurrently elevated, which enhances the contribution of accurate pseudo-labels to the consistency regularization loss.

Through Eq. (8), the standard branch provides pseudo-labels and consistency regularization weights to the balanced branch, further illustrating the interactions between the two branches. The predicted unlabeled distributions of both branches tend to converge, which will be showed in Sec. 4.5 and Fig. 5a.

3.4 Post-hoc Enhancement

Despite the efforts of the balanced branch \tilde{f} to achieve outstanding predictions for both head and tail classes, there

still exist some biases in \tilde{f} due to the unknown unlabeled data distribution, which will result in biased predictions when evaluating the model on the balanced test dataset. Consequently, we apply post-hoc enhancement to the model outputs to further improve model balance:

$$\tilde{q}_t(x) = \arg \max \tilde{f}(x) - \tau_b \cdot \log \tilde{\pi}, \quad (10)$$

where τ_b controls the balanced intensity for post-hoc enhancement. We utilize $\tilde{q}_t(x)$ as the final model’s prediction for sample x in the test dataset.

Why does not BOAT directly apply stronger logit adjustment (larger τ in Eq. (7)) to \tilde{f} to mitigate biases, but instead opt for post-hoc processing to further address the imbalance? In fact, during the training, stronger logit adjustment can lead to more incorrect pseudo-labels for unlabeled samples. These incorrect pseudo-labels inevitably impact training, especially representation learning. More discussion can be found in Sec. 4.5.

Algorithm 1 summarizes the whole framework of the proposed BOAT. The consistency regularizer for the standard branch is similar to FixMatch presented in Eq. (2). In general, each branch of the network has two losses to minimize, that is, the classification loss and the consistency regularizer. Put it together, our total objective function is:

$$\mathcal{L}_{\text{total}} = \underbrace{\mathcal{L}_{\text{labeled}} + \mathcal{L}_{\text{con}}}_{\text{standard branch}} + \underbrace{\mathcal{L}_{\text{b-labeled}} + \mathcal{L}_{\text{b-con}}}_{\text{balanced branch}}. \quad (11)$$

3.5 Distinctions with ACR

Although BOAT utilizes the dual-branch structure and logit adjustment to alleviate the imbalance issues in LTSSL tasks, which are similar to ACR, there still exists substantial upgrades to help BOAT to adapt to a broader range of LTSSL tasks and achieve better performance.

The main distinctions between ACR and BOAT are as follows:

- **Distribution Assumption.** ACR employs three typical anchor distributions to handle diverse unlabeled data, limiting its performance to *consistent*, *uniform*, and *reversed* scenarios. However, BOAT facilitates the dynamic convergence of the predictive distributions

TABLE 2

Test accuracy of previous LTSSL algorithms and our proposed BOAT under inconsistent class distributions, i.e., $\gamma_l \neq \gamma_u$, on CIFAR-10-LT and STL10-LT datasets. The γ_l is fixed to 100 for CIFAR-10-LT, while it is set to 10 and 20 for STL10-LT dataset. The best results are in **bold**.

Algorithm	CIFAR-10-LT ($\gamma_l \neq \gamma_u$)				STL10-LT ($\gamma_u = N/A$)			
	$\gamma_u = 1$ (uniform)		$\gamma_u = 1/100$ (reversed)		$\gamma_l = 10$		$\gamma_l = 20$	
	$N_1 = 500$ $M_1 = 4000$	$N_1 = 1500$ $M_1 = 3000$	$N_1 = 500$ $M_1 = 4000$	$N_1 = 1500$ $M_1 = 3000$	$N_1 = 150$ $M_1 = 100k$	$N_1 = 450$ $M_1 = 100k$	$N_1 = 150$ $M_1 = 100k$	$N_1 = 450$ $M_1 = 100k$
FixMatch [7]	73.0±3.81	81.5±1.15	62.5±0.94	71.8±1.70	56.1±2.32	72.4±0.71	47.6±4.87	64.0±2.27
w/ DARP [24]	82.5±0.75	84.6±0.34	70.1±0.22	80.0±0.93	66.9±1.66	75.6±0.45	59.9±2.17	72.3±0.60
w/ CReST [25]	83.2±1.67	87.1±0.28	70.7±2.02	80.8±0.39	61.7±2.51	71.6±1.17	57.1±3.67	68.6±0.88
w/ CReST+ [25]	82.2±1.53	86.4±0.42	62.9±1.39	72.9±2.00	61.2±1.27	71.5±0.96	56.0±3.19	68.5±1.88
w/ DASO [27]	86.6±0.84	88.8±0.59	71.0±0.95	80.3±0.65	70.0±1.19	78.4±0.80	65.7±1.78	75.3±0.44
w/ SimPro [29]	93.8±0.10	-	85.8±0.48	-	-	84.5±0.39	-	82.5±0.25
w/ ACR [28]	92.1±0.18	93.5±0.11	84.9±0.09	89.5±0.17	77.1±0.24	83.0±0.32	75.1±0.70	81.5±0.25
w/ Ours	93.9±0.02	94.1±0.08	86.6±0.33	89.9±0.21	83.3±0.46	86.6±0.15	82.1±0.52	85.7±0.53

TABLE 3

Test accuracy on CIFAR-100-LT dataset under *uniform* and *reversed* class distributions. The best results are in **bold**.

ALGORITHM	CIFAR-100-LT ($\gamma_l \neq \gamma_u$)			
	$\gamma_u = 1$ (UNIFORM)		$\gamma_u = 1/10$ (REVERSED)	
	$N_1 = 50$ $M_1 = 400$	$N_1 = 150$ $M_1 = 300$	$N_1 = 50$ $M_1 = 400$	$N_1 = 150$ $M_1 = 300$
FixMatch [7]	45.5±0.71	58.1±0.72	44.2±0.43	57.3±0.19
w/ DARP [24]	43.5±0.95	55.9±0.32	36.9±0.48	51.8±0.92
w/ CReST [25]	43.5±0.30	59.2±0.25	39.0±1.11	56.4±0.62
w/ CReST+ [25]	43.6±1.60	58.7±0.16	39.1±0.77	56.4±0.78
w/ DASO [27]	53.9±0.66	61.8±0.98	51.0±0.19	60.0±0.31
w/ ACR [28]	57.2±0.19	66.7±0.30	51.6±0.12	62.9±0.25
w/ Ours	60.4±0.72	68.0±0.21	53.3±0.20	63.5±0.22

Algorithm 1 The Proposed BOAT.

- 1: **Input:** labeled dataset \mathcal{D}^l and unlabeled dataset \mathcal{D}^u , standard branch f , balanced branch \tilde{f} , number of iterations T
- 2: **for** $t = 1$ **to** T **do**
- 3: $\{(x_i^{(l)}, y_i^{(l)})\}_{i=0}^{B-1} \leftarrow$ Sample a batch of labeled data
- 4: $\{x_j^{(u)}\}_{j=0}^{B-1} \leftarrow$ Sample a batch of unlabeled data
- 5: Update estimated class distribution $\tilde{\pi}$ by Eq. (5)
- 6: Generate the pseudo-labels $\tilde{q}(x_j^{(u)})$ for balanced branch
- 7: Obtain samples' weights via γ_t and $\eta(x_j^{(u)})$
- 8: Compute the $\mathcal{L}_{\text{labeled}}$ by Eq. (4)
- 9: Compute the $\mathcal{L}_{\text{b-labeled}}$ by Eq. (3)
- 10: Compute the \mathcal{L}_{con} by Eq. (2)
- 11: Compute the $\mathcal{L}_{\text{b-con}}$ by Eq. (8)
- 12: Compute the total loss $\mathcal{L}_{\text{total}}$ by Eq. (11)
- 13: Update f and \tilde{f} based on $\nabla \mathcal{L}_{\text{total}}$ using SGD
- 14: **end for**

of the two branches without any assumptions about the unlabeled distribution.

- **Adjustment strategy.** In order to alleviate biases introduced by the imbalanced distribution, ACR performs logit adjustment on predictions of unlabeled data according to the distribution of labeled data, which differs significantly from the real distribution of unlabeled data, leading to poor performance. Conversely, BOAT adjusts model predictions by the estimated distribution from f , which can dynamically

reflect the model's inclination as training progresses, thus enhancing the versatility and performance of the model.

- **Selection of pseudo-labels.** ACR only uses a fixed threshold to filter out less confident pseudo-labels, while BOAT weights the consistency loss of \tilde{f} based on adjustments of outputs from f , mitigating the impact of erroneous pseudo-labels with excessive tail shift on training during logit adjustment.
- **Further improvement during inference.** BOAT employs post-hoc enhancement to further boost performance significantly, whereas ACR, due to over-balancing during the training, fails to gain considerable performance enhancement through post-hoc enhancement. More details can be found in Sec. 4.5.

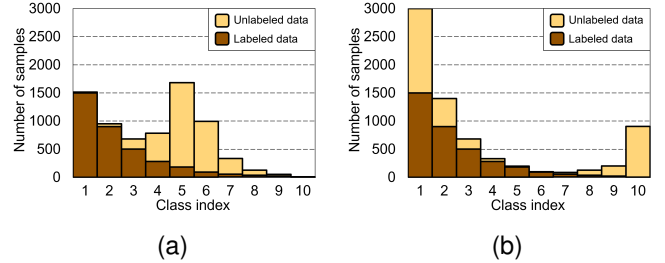


Fig. 2. More class distribution patterns for unlabeled data, i.e., *middle* and *headtail*.

TABLE 4

Test accuracy on ImageNet-127. The best results are in **bold**.

Algorithm	32×32	64×64
FixMatch [7]	29.7	42.3
w/ DARP [24]	30.5	42.5
w/ DARP+cRT [24]	39.7	51.0
w/ CReST+ [25]	32.5	44.7
w/ CReST++LA [31]	40.9	55.9
w/ CoSSL [36]	43.7	53.9
w/ SimPro [29]	59.1	67.0
w/ ACR [28]	57.2	63.6
w/ Ours	60.5	68.4

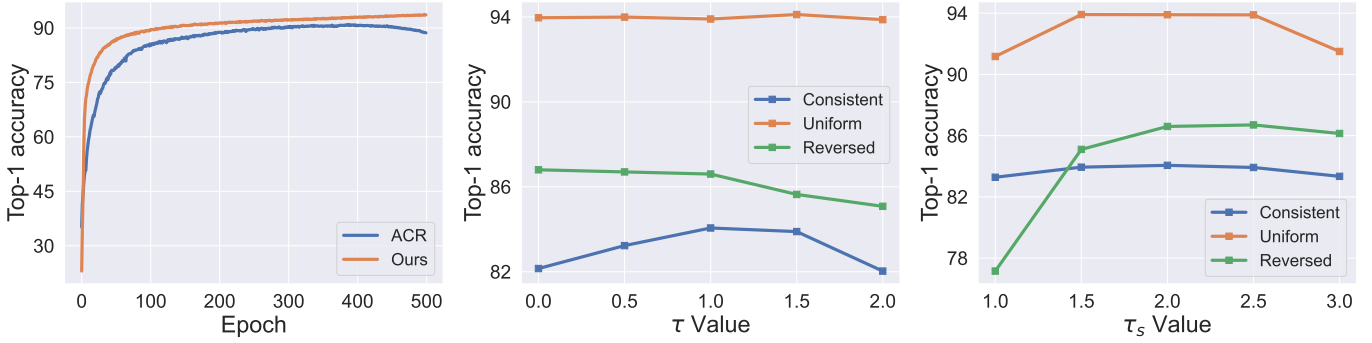


Fig. 3. (3a): Pseudo-label accuracy for unlabeled data. The reported results are based on the average accuracy of *consistent*, *uniform*, and *reversed* with $\gamma_l = 100$ on CIFAR-10-LT. (3b and 3c): The sensitivity of τ and τ_s under various settings on CIFAR-10-LT.

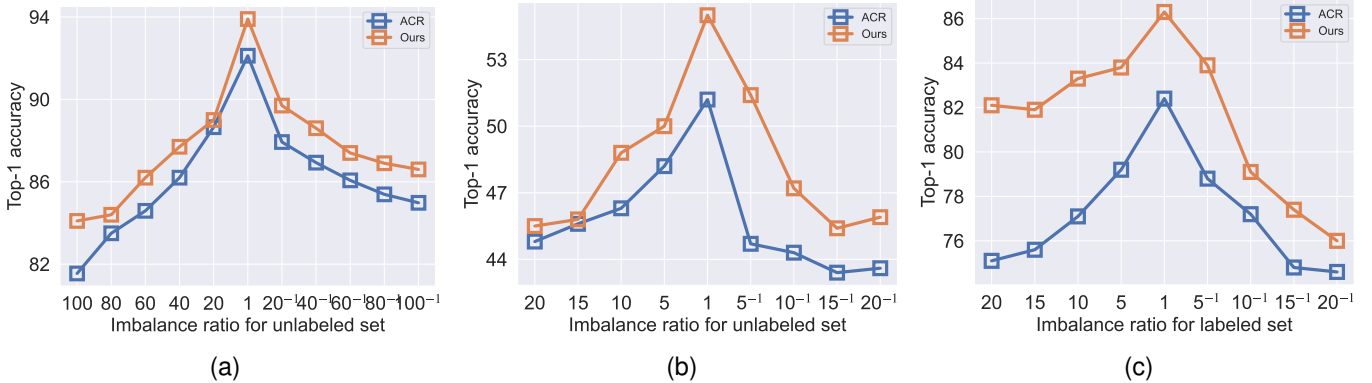


Fig. 4. More realistic LTSSL settings with various imbalance ratio for unlabeled data or labeled data. (4a): $N_1 = 500, M_1 = 4000$ with $\gamma_l = 100$ on CIFAR-10-LT. (4b): $N_1 = 50, M_1 = 400$ with $\gamma_l = 20$ on CIFAR-100-LT. (4c): $N_1 = 150$ with various imbalanced ratio for labeled set on STL10-LT.

TABLE 5

Test accuracy on CIFAR-10-LT and CIFAR-100-LT dataset under *middle* and *headtail* settings. We set $N_1 = 500, M_1 = 4000$ for CIFAR-10-LT and $N_1 = 50, M_1 = 400$ for CIFAR-100-LT. The best results are in **bold**.

Algorithm	CIFAR-10-LT ($\gamma_l = 100$)		CIFAR-100-LT ($\gamma_l = 20$)	
	$\gamma_u = 100$		$\gamma_u = 20$	
	middle	headtail	middle	headtail
FixMatch [7]	71.7 ± 0.46	66.6 ± 0.87	39.7 ± 0.61	38.2 ± 0.82
w/ CReST+ [25]	71.4 ± 0.60	67.2 ± 0.48	36.9 ± 0.57	35.1 ± 1.10
w/ DASO [27]	73.1 ± 0.68	71.1 ± 0.32	43.1 ± 1.20	43.8 ± 0.43
w/ SimPro [29]	84.8 ± 0.54	83.0 ± 0.36	43.6 ± 0.35	44.8 ± 0.56
w/ ACR [28]	83.2 ± 0.41	80.6 ± 0.30	44.6 ± 0.25	42.3 ± 0.17
w/ Ours	86.8 ± 0.54	83.1 ± 0.04	45.7 ± 0.34	44.9 ± 0.53

4 EXPERIMENTS

We conduct extensive experiments to demonstrate the effectiveness of the proposed BOAT under various class distributions of unlabeled data.

4.1 Experimental setup

The experiments we conducted are based on widely used datasets, including CIFAR-10-LT [44], CIFAR-100-LT [44], STL10-LT [45], and ImageNet-127 [36]. Recall that parameter γ_l is used to control the imbalance ratio of the labeled dataset, and we can decide the number of labeled samples for class c as $N_c = N_1 \cdot \gamma_l^{-\frac{c-1}{C-1}}$ once N_1 is given. Likewise,

given the imbalance ratio of unlabeled dataset γ_u and M_1 (or M_C in the *reversed* setting), we set M_c as we did for the labeled dataset.

- **CIFAR-10-LT**: Following DASO [27], we test our method under $N_1 = 500, M_1 = 4000$ and $N_1 = 1500, M_1 = 3000$ settings. We report results with imbalance ratios $\gamma_l = \gamma_u = 100$ and $\gamma_l = \gamma_u = 150$. For *uniform* and *reversed* settings, we fix $\gamma_l = 100$ and adjust $\gamma_u \in \{1, 1/100\}$ to simulate various class distribution of unlabeled data.
- **CIFAR-100-LT**: We test our method under $N_1 = 50, M_1 = 400$ and $N_1 = 150, M_1 = 300$ settings. The imbalance ratio is set to $\gamma_l = \gamma_u = 10$ and $\gamma_l = \gamma_u = 20$. With a fixed $\gamma_l = 10$, we also test our method under $\gamma_u \in \{1, 1/10\}$ for the *uniform* and *reversed* unlabeled data class distributions.
- **STL10-LT**: Since ground-truth labels of unlabeled data in STL-10 are unknown, we conduct experiments by controlling the imbalance ratio of labeled data. We follow the settings by DASO and set $\gamma_l \in \{10, 20\}$.
- **ImageNet-127**: ImageNet127 is a naturally long-tailed dataset, so we do not need to construct the datasets manually. Following CoSSL [36], we down-sample the image size to 32×32 and 64×64 due to limited resources.

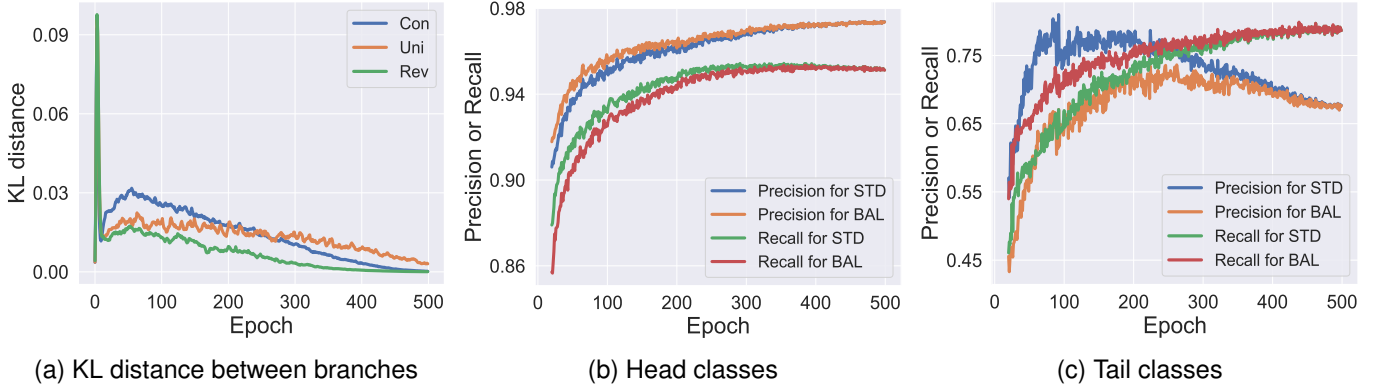


Fig. 5. (5a): The KL distance of predicted unlabeled data distribution between standard and balanced branch. The experiments are conducted on CIFAR-100-LT with $N_1 = 50, M_1 = 400$, and $\gamma_l = 10$. *Con*, *Uni*, and *Rev* represent *consistent*, *uniform*, and *reversed* for short. (5b and 5c): The average precision and recall across different settings for head and tail classes. The experiments are conducted on CIFAR-10-LT with $N_1 = 500, M_1 = 4000$, and $\gamma_l = 100$. *STD* and *BAL* represent standard branch and balanced branch, respectively.

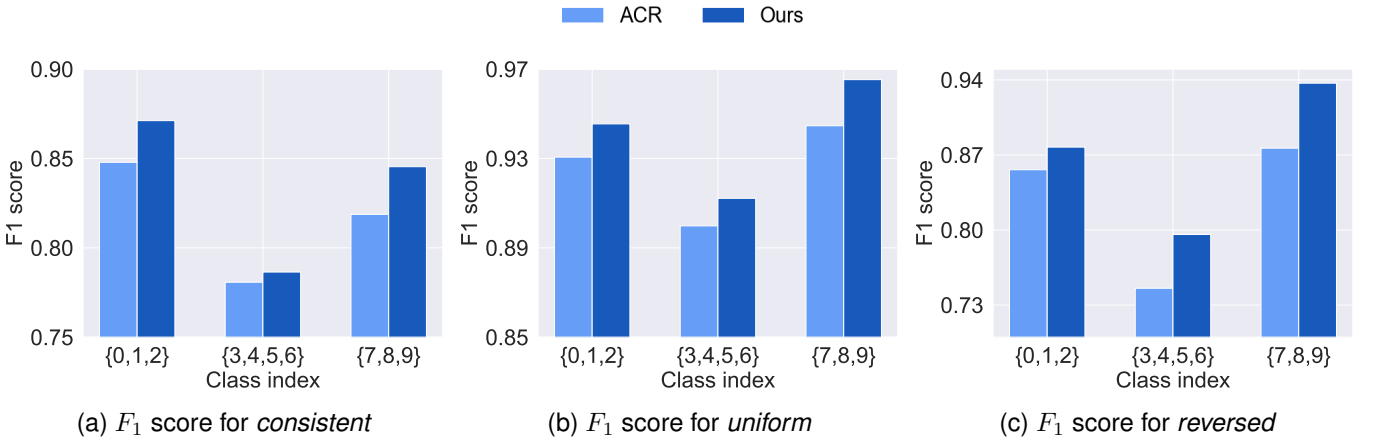


Fig. 6. The comparison of F_1 score for ACR and BOAT on CIFAR-10-LT with $N_1 = 500, M_1 = 4000$ and $\gamma_l = 100$.

Following previous work [36], [46], we implement our method using Wide ResNet-28-2 [47] on CIFAR-10-LT, CIFAR-100-LT, and STL10-LT; and ResNet-50 on ImageNet-127. Following FixMatch, we train the network for 500 epochs with 500 mini-batches in each epoch, with a batch size of 64, using standard SGD with momentum [48], [49], [50]. We use a cosine learning rate decay [51] which sets the learning rate to $\eta \cos(\frac{\gamma \pi t}{16T})$, where η is the initial learning rate, t is the current training step, and T is the total number of training steps. We set $\tau_s = 2.0$ for all datasets which is defined in Eq. (4), and when considering τ , we fix it to 1.0 except on CIFAR-100-LT where it is set to 2.0. For post-hoc enhancement, τ_b is set to 2.0 for CIFAR-10-LT while setting it to 1.0 for the remaining datasets. To demonstrate the superiority of our BOAT we compare with many existing LTSSL algorithms, including DARP [24], CReST [25], DASO [27], ABC [21], TRAS [23], SimPro [29], and ACR [28]. We measure the performance of all methods using the top-1 accuracy in the test set. We report each method’s mean and standard deviation of three independent runs in our experiments. Following [7], we report final performance from balanced branch f using an exponential moving average of model parameters. All experiments can be conducted in PyTorch with a single NVIDIA V100 32GB GPU.

4.2 Results on CIFAR10/100-LT and STL10-LT

We first evaluate the performance when the class distributions are *consistent* (i.e., $\gamma_l = \gamma_u$) in Tab. 1. Subsequently, in Tab. 2 and Tab. 3, we report results when the unlabeled data class distribution is *uniform* or *reversed* (e.g., $\gamma_u = 1$ or $\gamma_u = 1/100$). It is noteworthy that the distribution of unlabeled data in STL10-LT is completely unknown.

In case of $\gamma_l = \gamma_u$. We compare our approach ACR with several state-of-the-art LTSSL methods: DARP [24], CReST+ [25], DASO [27], SimPro [29], and ACR [28]. Results are reported in Table 1. Without exception, BOAT consistently outperforms existing methods by a large margin, even though some of these methods are particularly developed based on the assumption that labeled and unlabeled data share the same class distribution. This observation verifies the superior performance of our method. Specifically, BOAT exhibits a 1.9% average advantage over ACR, particularly excelling on the CIFAR-10-LT where the average advantage reaches 3.1%.

In case of $\gamma_l \neq \gamma_u$. In real-world datasets, the class distribution of unlabeled data is likely to be significantly inconsistent with labeled data. Therefore, we consider *uniform* and *reversed* class distributions, e.g., $\gamma_u = 1$ or $\gamma_u = 1/100$ for CIFAR-10-LT. On the STL10-LT dataset, due to the unknown

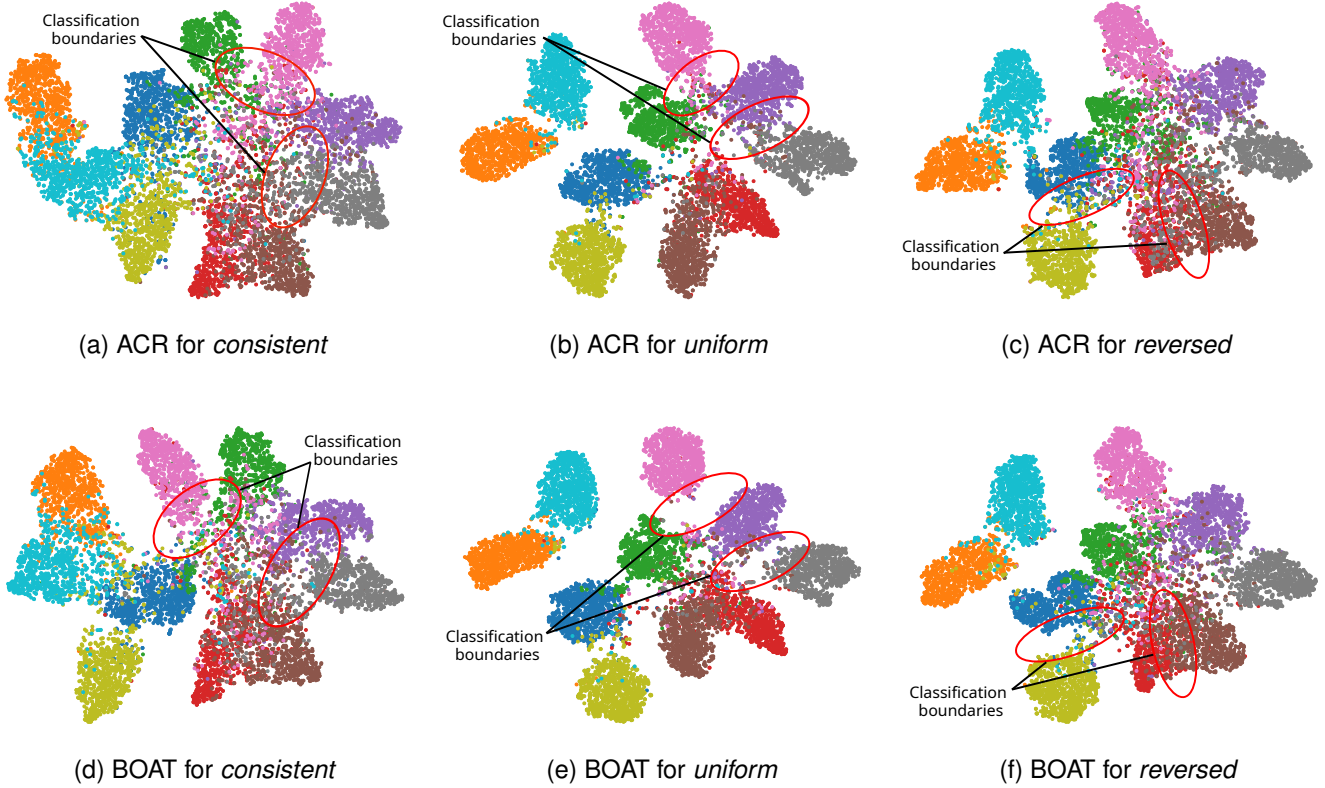


Fig. 7. The t-SNE visualization of the test set for ACR and BOAT on CIFAR-10-LT with $N_1 = 500$, $M_1 = 4000$ and $\gamma_l = 100$.

ground-truth labels of the unlabeled data, we can only control the imbalance ratio of labeled data. The results are summarized in the Tab. 2 and Tab. 3.

It can be seen that BOAT achieves the best results when the class distributions of unlabeled data are inconsistent. For example, BOAT obtains 16.8% and 21.1% absolute performance gains over FixMatch under $\gamma_u = 1$ and $\gamma_u = 1/100$ on CIFAR-10-LT, respectively. Similarly, the CIFAR-100-LT results show that our method outperforms ACR by an average of 1.7% accuracy increase. For STL10-LT, BOAT achieves the best results with averaged 5.3% accuracy gain compared with ACR, even if the unlabeled data distribution is unknown. Generally speaking, empirical results under unknown class distributions of unlabeled data on three datasets justify that BOAT can effectively utilize unlabeled data to alleviate the negative impact of class imbalance.

4.3 Results on ImageNet-127

ImageNet127 is initially introduced in previous work [52] and is applied to LTSSL by CREST [25], which groups the 1000 classes of ImageNet [53] into 127 classes based on the WordNet hierarchy. Compared with other datasets, we do not need to construct the dataset artificially because it naturally follows a long-tailed class distribution with an imbalance ratio $\gamma \approx 286$. Following CoSSL [36], we down-sample the original images to smaller sizes of 32×32 or 64×64 pixels using the box method from the Pillow library and randomly select 10% training samples to form the labeled set. It is worth noting that the test set of ImageNet-127 is also long-tailed. The results are summarized in Tab. 4.

We can see that BOAT achieves superior results for both image sizes 32×32 and 64×64 with 3.3% and 4.8% absolute improvement on test accuracy compared with ACR [28], respectively. The results show that BOAT can be successfully applied to tasks with long-tailed test datasets.

4.4 Results under more class distributions

To examine the performance of our method in more imbalanced scenarios, we conduct additional experiments on CIFAR-10-LT (CIFAR-100-LT) by fixing $\gamma_l = 100$ ($\gamma_l = 20$) while varying the imbalance ratio of unlabeled data γ_u from *consistent* to *reversed* by a step size 20 (step size 5). We set $N_1 = 500$ and $M_1 = 4000$ ($N_1 = 50$ and $M_1 = 400$) ($M_C = 4000$ ($M_C = 400$) in *reversed* setting) and compare the performance with ACR [28]. The results are reported in Fig. 4. It can be easily observed that our method BOAT consistently outperforms ACR in all test cases. The performance gain becomes increasingly significant as the class distribution of unlabeled data changes from *consistent* to *reversed* on CIFAR-100-LT. In addition, for STL10-LT, we find that BOAT can also achieve impressive performance under various imbalanced labeled ratio in Fig. 4c. This demonstrates the capability of our method to handle various realistic LTSSL problems adaptively.

In addition, SimPro [29] introduces two more class distribution patterns for unlabeled data, i.e., *middle* and *headtail*, which are illustrated in Fig. 2. The middle distribution represents a concentration of classes in the middle range of labeled data’s classes, whereas the head-tail distribution indicates a concentration at both extremes. The results are

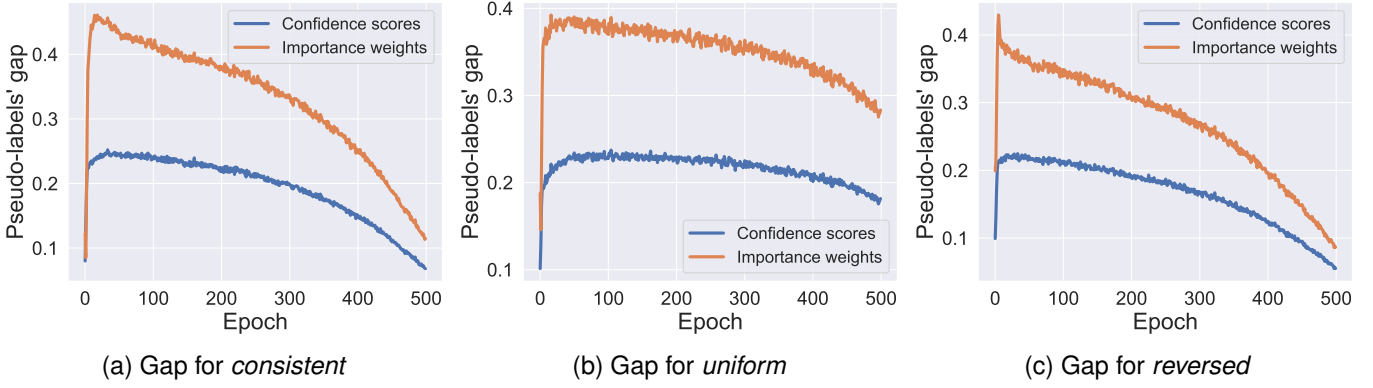


Fig. 8. The confidence scores and importance weights gap between accurate and incorrect pseudo-labels of different settings. The experiments are conducted on CIFAR-100-LT with $N_1 = 50$, $M_1 = 400$, and $\gamma_l = 10$.

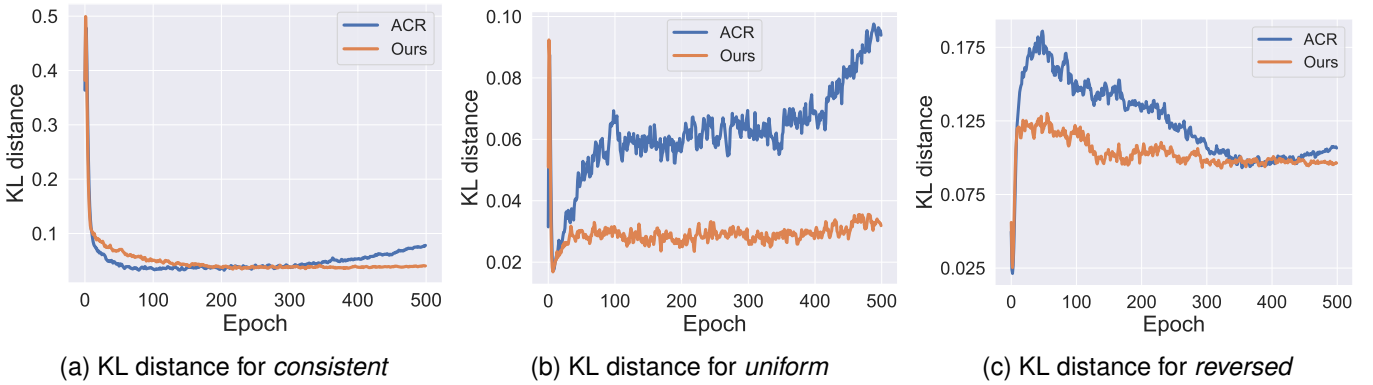


Fig. 9. The KL distance between the predicted and true distributions of the unlabeled data. The experiments are conducted on CIFAR-100-LT with $N_1 = 50$, $M_1 = 400$, and $\gamma_l = 10$.

TABLE 6

The comparison between ACR and BOAT of post-hoc enhancement for different τ_b . The experiments are conducted on CIFAR-10-LT with $\gamma_l = 100$, $N_1 = 500$, $M_1 = 4000$.

Algorithm	CIFAR-10-LT		
	$\gamma_u = 100$	$\gamma_u = 1$	$\gamma_u = 1/100$
ACR [28] ($\tau_b = 0$)	81.6 ± 0.19	92.1 ± 0.18	84.9 ± 0.09
w/ $\tau_b = 1$	82.4 ± 0.45	92.1 ± 0.17	85.4 ± 0.19
w/ $\tau_b = 2$	82.0 ± 0.42	92.2 ± 0.21	86.0 ± 1.23
BOAT ($\tau_b = 0$)	77.8 ± 0.43	93.8 ± 0.01	85.5 ± 0.33
w/ $\tau_b = 1$	82.3 ± 0.44	93.8 ± 0.03	86.3 ± 0.26
w/ $\tau_b = 2$	84.1 ± 0.56	93.9 ± 0.02	86.6 ± 0.33

reported in Tab. 5, and we note that BOAT achieves an average performance improvement of 1.1% compared to SimPro, suggesting that our method can adapt to arbitrary distributions of unlabeled data without assuming any prior unlabeled distribution.

4.5 Systematic analysis of the proposed method

To better understand our method, we conduct extensive studies to demonstrate the effectiveness of BOAT.

Quality of pseudo-labels. Fig. 3a illustrates the accuracy of pseudo-labels between ACR and BOAT. It is noteworthy that BOAT consistently exhibits higher accuracy during training

TABLE 7

Ablation studies of our proposed BOAT algorithm. *Con*, *Uni*, and *Rev* represent *consistent*, *uniform*, and *reversed* for short.

Ablations	CIFAR-10-LT			CIFAR-100-LT		
	Con	Uni	Rev	Con	Uni	Rev
Ours	84.1	93.9	86.6	52.0	60.4	53.3
w/o alignment	84.2	84.6	66.8	51.9	60.2	50.1
w/o balanced pseudo-labels	82.2	93.9	86.2	51.7	58.0	49.9
w/o balanced softmax	84.0	93.5	86.1	51.1	59.6	52.7
w/o weighting	83.8	93.3	86.5	51.8	58.3	52.1

compared to ACR, and it is obvious that pseudo-labels' accuracy plays a pivotal role in enhancing the performance of SSL tasks [12].

The iterative convergence of standard and balanced branch. In our proposed BOAT, the standard branch focuses on enhancing performance for head classes while the balanced branch aims to improve performance for tail classes. Both branches progressively converge during training, ultimately achieving satisfactory performance across both head and tail classes. Fig. 5a shows that, across different settings, the distance between the predicted unlabeled data distribution of the two branches progressively decreases, indicating that the branches are converging towards one another. In addition, we present the precision and recall of

TABLE 8

The results are based on fine-tuning the pre-trained CLIP model. The fine-tuning strategies employed in the experiments are visual prompt tuning (VPT) [54] and AdaptFormer [55]. We set $N_1 = 500, M_1 = 4000, \gamma_l = 100$ for CIFAR-10-LT, $N_1 = 50, M_1 = 400, \gamma_l = 10$ for CIFAR-100-LT, and $N_1 = 150$ for STL10-LT.

Algorithm	CIFAR-10-LT			CIFAR100-LT			STL10-LT	
	Con	Uni	Rev	Con	Uni	Rev	$\gamma_l = 10$	$\gamma_l = 20$
FixMatch + VPT [54]	92.8 ± 0.22	95.1 ± 0.11	95.2 ± 0.65	78.6 ± 0.65	81.3 ± 0.44	79.7 ± 0.21	98.4 ± 0.04	97.3 ± 0.42
w/ ACR [28]	95.5 ± 0.54	97.1 ± 0.05	96.2 ± 0.42	80.8 ± 0.20	81.2 ± 0.23	80.3 ± 0.34	98.2 ± 0.14	97.8 ± 0.78
w/ Ours	96.0 ± 0.30	97.3 ± 0.29	96.7 ± 0.34	81.3 ± 0.21	82.9 ± 0.15	81.9 ± 0.23	98.7 ± 0.25	98.5 ± 0.23
FixMatch + Adaptformer [55]	92.7 ± 0.23	95.6 ± 0.15	95.8 ± 0.11	79.7 ± 0.45	81.7 ± 0.23	80.2 ± 0.45	98.4 ± 0.30	98.3 ± 0.23
w/ ACR [28]	96.1 ± 0.33	97.6 ± 0.23	96.2 ± 0.76	81.7 ± 0.56	83.3 ± 0.65	81.4 ± 0.38	98.6 ± 0.52	98.4 ± 0.45
w/ Ours	96.7 ± 0.41	97.8 ± 0.25	96.8 ± 0.34	82.2 ± 0.13	83.6 ± 0.32	83.1 ± 0.19	98.6 ± 0.56	98.9 ± 0.20

pseudo-labels for head and tail classes in Figs. 5b and 5c. Regarding the head classes, it is noted that the standard branch exhibits lower precision but higher recall compared to the balanced branch during the training, which indicates that the standard branch tends to favor the head classes [56]. Similarly, regarding the tail classes, the balanced branch shows lower precision and higher recall, suggesting its inclination towards the tail classes. In line with our expectations, the differences in precision and recall between the two branches reduced progressively for head and tail classes during the training. Simultaneously, there exists a general upward trend for most precision and recall, demonstrating that both branches are converging and achieving improved performance for all classes. The precision for tail classes exhibits a declining trend in later stages, and we attribute this to the expected phenomenon of tailward inclination, which helps mitigate the bias introduced by long-tailed distributions in the dataset. In conjunction with Fig. 3a, we can conclude that as the two branches progressively converge, the accuracy of pseudo-labels continually increases, thus improving the generalization performance of our model.

Benefits for all classes. The two branches in our proposed BOAT gradually converge during the training, ultimately achieving commendable performance across all classes. As illustrated in Fig. 6, we observe that BOAT can achieve higher F_1 score for various settings when compared to ACR on test dataset. Specifically, whether in head or tail classes, BOAT exhibits commendable F_1 scores, indicating its ability to enhance tail classes performance while preserving advantages in head classes.

Hyperparameter sensitivity. Despite the commendable performance achieved by our method, the inclusion of certain crucial parameters necessitates an examination of whether the exceptional results are solely due to parameter tuning. Therefore, we explore the sensitivity of τ and τ_s in Fig. 3. τ in Eq. (7) controls the logit adjustment intensity for the balanced branch’s pseudo-labels. Our observations indicate marginal fluctuations in performance for both *consistent* and *reversed*, while the performance of *uniform* displays a stable tendency. Generally, when τ equals 1, better overall performance can be achieved. When considering τ_s , we find that lower values result in poorer performance for *reversed*. We attribute this to the significant distribution disparities between labeled and unlabeled data, and higher τ_s can provide strong balancing intensity to alleviate biases introduced by labeled data and shift towards the real distribution of

unlabeled data. Therefore, we set $\tau_s = 2$ in our experiments.

Representation visualization. We visualize the learned representations of BOAT using the t-distributed stochastic neighbor embedding (t-SNE) [57] and compare them with ACR. Fig. 7 illustrates the comparison results on test set under *consistent*, *uniform*, and *reversed* settings. It can be seen from the figure that the representations obtained by BOAT allow for clearer classification boundaries, which can further enhance the model’s performance in classification.

Why post-hoc enhancement is needed? To illustrate the necessity of post-hoc enhancement for BOAT, Tab. 6 compares the performance effects of various enhancement intensities between ACR and BOAT. Upon removing post-hoc enhancement ($\tau_b = 0$), we noticed the BOAT didn’t exhibit substantial performance benefits and even performed 3.8% worse than ACR under *consistent*. However, with the inclusion of post-hoc enhancement ($\tau_b = 2$), BOAT shows a notable enhancement in performance averaging at 2.5%, contrasting with the marginal 0.5% improvement of ACR. We attribute this superior performance to more attention of BOAT on the accuracy of pseudo-labels during the training. As depicted in Fig. 3a, BOAT achieves higher pseudo-label accuracy compared to ACR, without overbalancing the model, thus possessing more significant potential for performance improvement through post-hoc enhancement. In contrast, ACR’s strong logit adjustment during training introduces more erroneous pseudo-labels, hindering representation learning as evident in Fig. 7 and consequently limiting the extent of performance gains achievable through post-hoc enhancement. Based on these results and findings, we conclude that an effective LTSSL model should prioritize enhancing the accuracy of pseudo-labels during the training. This prioritization ensures that the model possesses a robust foundation for subsequent performance improvement through post-hoc enhancement.

The role of samples’ weights. During the optimization of the consistency regularizer in the balanced branch, we assign weight $\psi(x_j^{(u)})$ to the sample $x_j^{(u)}$. We hope to prioritize correct pseudo-labels with higher weights and give lower weights to incorrect samples. Therefore, we first define the gap between accurate and incorrect pseudo-labels:

$$\psi_{gap} = \frac{1}{|\mathcal{U}^+|} \sum_{x_j^{(u)} \in \mathcal{U}^+} \psi(x_j^{(u)}) - \frac{1}{|\mathcal{U}^-|} \sum_{x_j^{(u)} \in \mathcal{U}^-} \psi(x_j^{(u)}) \quad (12)$$

where $\mathcal{U}^+ = \{x_j^{(u)} \mid \tilde{q}_j = y_j^{(u)}, x_j^{(u)} \in \mathcal{D}^u\}$ and $\mathcal{U}^- =$

$\{x_j^{(u)} \mid \tilde{q}_j \neq y_j^{(u)}, x_j^{(u)} \in \mathcal{D}^u\}$ represent the collections of unlabeled samples with accurate and incorrect pseudo-labels, respectively. $y_j^{(u)}$ is the real label for unlabeled sample $x_j^{(u)}$. It is evident that we hope the disparity in weights between accurate and incorrect pseudo-labels is significant, so ψ_{gap} should be as large as possible. To confirm the superiority of sample weights, we can also calculate the gap in confidence scores between accurate and incorrect pseudo-labels. The results are shown in Fig. 8, and we can conclude that sample weights exhibit a larger gap compared to confidence scores across all settings, indicating that sample weights can more easily distinguish between accurate and incorrect pseudo-labels, thus mitigating the damage to the model’s performance caused by erroneous pseudo-labels.

Estimation of unlabeled data distribution. In our method, the alignment of the unlabeled data distribution in Eq. (4) and the adjustments made during post-hoc enhancement both demonstrate that the accuracy of the predicted unlabeled data distribution $\tilde{\pi}$ is critical to the performance of BOAT. Therefore, we present the KL distance between the predicted distribution and the true unlabeled data distribution for different scenarios in Fig. 9. Evidently, as training progresses, BOAT achieves more accurate distribution prediction $\tilde{\pi}$ compared to ACR, which is significantly beneficial for improving the performance of BOAT.

4.6 Ablation Analysis

To better understand BOAT, we tease apart the factors that contribute significantly to its success in Table 7.

Impact of alignment. The distribution alignment in Eq. (4) aims to leverage the correct label information from the labeled data to guide the predictions of the standard branch to align more closely with the inclination of the balanced branch. Without alignment, the labeled portion of the standard branch loss will be directly calculated using cross-entropy, which will consistently be influenced by biases introduced by imbalanced labeled data. In our experiments, we notice a significant performance decline upon removing the alignment, especially for *uniform* and *reversed*, averaging 8.1%. The phenomenon suggests that alignment can effectively steer the model in the correct direction without being skewed by imbalanced labeled data.

Impact of balanced pseudo-labels. In our proposed BOAT, the balanced branch employs pseudo-labels from the standard branch after the adjustment by Eq. (7). If we remove the adjustment, we observe a decrease averaged 1.4% in accuracy across all settings, indicating that balanced pseudo-labels can effectively aid the balanced branch in mitigating bias towards head classes while maintaining high performance on tail classes.

Impact of balanced softmax. The balanced softmax in Eq. (3) effectively mitigates the issue of labeled data imbalance within the balanced branch, leading to more balanced predictions. The exclusion of the balanced softmax results in an average performance drop of 0.6% across all settings, emphasizing the necessity of incorporating the balanced softmax into the labeled loss in balanced branch.

Impact of weighting. In consistency regularizer for balanced branch in Eq. (8), we employ importance weights to evaluate the reliability of pseudo-labels. From the Tab. 7, we

observe a decrease in accuracy averaged 0.7%, suggesting that importance weights can effectively filter out unstable pseudo-labels and enhance the model’s performance.

4.7 Looking ahead: future LTSSL methods

While BOAT has achieved outstanding performance, we have observed that recent popular foundation model [58] can achieve excellent performance on downstream tasks through fine-tuning [59], [60], [61], [62]. Therefore, we investigate whether fine-tuning foundation models can further enhance the performance of the LTSSL method. We choose CLIP [58] for fine-tuning due to its strong generalization ability. CLIP is a multimodal model to align images and text in a shared embedding space, facilitating tasks like image classification, generation, and zero-shot learning across various domains [60]. When considering full fine-tuning the model, the target tasks often require a substantial amount of data for effective adaptation [63], [64]. However, for LTSSL tasks, labeled data is scarce and severely imbalanced, hindering full fine-tuning from achieving satisfactory performance. Therefore, motivated by [60], we attempt to leverage the parameter-efficient fine-tuning (PEFT) strategy [54], [55], [65] for fine-tuning to enhance the generalization performance of LTSSL models. PEFT strategies always freeze the pre-trained model while introducing a few learnable parameters for the adaptation. The results are shown in Tab. 8, and we utilize Visual Prompt Tuning (VPT) [54] and AdaptFormer [55] for fine-tuning. VPT prepends learnable prompts optimized during the training at each transformer layer. AdaptFormer adds a bottleneck module, which is parallel to the FFN layer. The incorporation of VPT and AdaptFormer facilitates a notable 17.6% and 18.2% performance improvement for BOAT compared to the Wide ResNet-based model [47]. Additionally, we find that BOAT outperforms ACR by 0.6% when employing PEFT fine-tuning on CIFAR-10-LT and CIFAR-100-LT, further demonstrating the broad applicability of BOAT. Regarding the STL10-LT, we observe that the performance of all methods has almost saturated, with error rates generally below 2%. Given the substantial performance gains achieved through fine-tuning foundation models with PEFT, we advocate for adopting PEFT fine-tuning as promising strategies for addressing LTSSL challenges in the future.

5 CONCLUSION

This paper presents a simple and effective method BOAT by minimizing the adaptive consistency regularizer for long-tailed semi-supervised learning with unknown class distributions of the unlabeled data. To ensure the high accuracy of the pseudo-labels, we utilize a double-branch network to guarantee the precision of head and tail classes individually. During the training, the two branches are iteratively aligned through interactions, ultimately achieving satisfactory accuracy across all classes. We implement the interactions by adjustments to the pseudo-labels and alignment to estimated distribution between two branches. We empirically show that our method significantly outperforms all competing methods under various scenarios, offering a solid baseline for future studies in this task.

REFERENCES

- [1] K. He, X. Zhang, S. Ren, and J. Sun, "Deep residual learning for image recognition," in *Proceedings of the IEEE conference on computer vision and pattern recognition*, 2016, pp. 770–778.
- [2] A. Krizhevsky, I. Sutskever, and G. E. Hinton, "Imagenet classification with deep convolutional neural networks," *Communications of the ACM*, vol. 60, no. 6, pp. 84–90, 2017.
- [3] D. Amodei, S. Ananthanarayanan, R. Anubhai, J. Bai, E. Battenberg, C. Case, J. Casper, B. Catanzaro, Q. Cheng, G. Chen *et al.*, "Deep speech 2: End-to-end speech recognition in english and mandarin," in *International conference on machine learning*. PMLR, 2016, pp. 173–182.
- [4] A. Tarvainen and H. Valpola, "Mean teachers are better role models: Weight-averaged consistency targets improve semi-supervised deep learning results," *Advances in Neural Information Processing Systems*, vol. 30, pp. 1195–1204, 2017.
- [5] T. Miyato, S.-i. Maeda, M. Koyama, and S. Ishii, "Virtual adversarial training: a regularization method for supervised and semi-supervised learning," *IEEE Transactions on Pattern Analysis and Machine Intelligence*, vol. 41, no. 8, pp. 1979–1993, 2018.
- [6] D. Berthelot, N. Carlini, I. Goodfellow, N. Papernot, A. Oliver, and C. A. Raffel, "Mixmatch: A holistic approach to semi-supervised learning," *Advances in Neural Information Processing Systems*, vol. 32, pp. 5050–5060, 2019.
- [7] K. Sohn, D. Berthelot, N. Carlini, Z. Zhang, H. Zhang, C. A. Raffel, E. D. Cubuk, A. Kurakin, and C.-L. Li, "Fixmatch: Simplifying semi-supervised learning with consistency and confidence," *Advances in Neural Information Processing Systems*, vol. 33, pp. 596–608, 2020.
- [8] Q. Xie, Z. Dai, E. H. Hovy, T. Luong, and Q. Le, "Unsupervised data augmentation for consistency training," in *Advances in Neural Information Processing Systems*, 2020.
- [9] T. Wei and Y.-F. Li, "Does tail label help for large-scale multi-label learning?" *IEEE Transactions on Neural Networks and Learning Systems*, vol. 31, no. 7, pp. 2315–2324, 2019.
- [10] B. Zhang, Y. Wang, W. Hou, H. Wu, J. Wang, M. Okumura, and T. Shinozaki, "Flexmatch: Boosting semi-supervised learning with curriculum pseudo labeling," *NeurIPS*, vol. 34, pp. 18 408–18 419, 2021.
- [11] Y. Wang, H. Chen, Q. Heng, W. Hou, Y. Fan, Z. Wu, J. Wang, M. Savvides, T. Shinozaki, B. Raj *et al.*, "Freematch: Self-adaptive thresholding for semi-supervised learning," *arXiv preprint*, 2022.
- [12] H. Chen, R. Tao, Y. Fan, Y. Wang, J. Wang, B. Schiele, X. Xie, B. Raj, and M. Savvides, "Softmatch: Addressing the quantity-quality trade-off in semi-supervised learning," *arXiv preprint*, 2023.
- [13] B. Zhou, Q. Cui, X.-S. Wei, and Z.-M. Chen, "Bbn: Bilateral-branch network with cumulative learning for long-tailed visual recognition," in *Proceedings of the IEEE/CVF conference on computer vision and pattern recognition*, 2020, pp. 9719–9728.
- [14] L. Xiang, G. Ding, and J. Han, "Learning from multiple experts: Self-paced knowledge distillation for long-tailed classification," in *European Conference on Computer Vision*. Springer, 2020, pp. 247–263.
- [15] X. Wang, L. Lian, Z. Miao, Z. Liu, and S. X. Yu, "Long-tailed recognition by routing diverse distribution-aware experts," *arXiv preprint arXiv:2010.01809*, 2020.
- [16] J. Li, Z. Tan, J. Wan, Z. Lei, and G. Guo, "Nested collaborative learning for long-tailed visual recognition," in *Proceedings of the IEEE/CVF Conference on Computer Vision and Pattern Recognition*, 2022, pp. 6949–6958.
- [17] J. Cui, Z. Zhong, S. Liu, B. Yu, and J. Jia, "Parametric contrastive learning," in *Proceedings of the IEEE/CVF international conference on computer vision*, 2021, pp. 715–724.
- [18] Z. Liu, Z. Miao, X. Zhan, J. Wang, B. Gong, and S. X. Yu, "Large-scale long-tailed recognition in an open world," in *Proceedings of the IEEE/CVF Conference on Computer Vision and Pattern Recognition*, 2019, pp. 2537–2546.
- [19] T. Wei, J. Shi, W. Tu, and Y. Li, "Robust long-tailed learning under label noise," *CoRR*, vol. abs/2108.11569, 2021.
- [20] B. Zhu, Y. Niu, X.-S. Hua, and H. Zhang, "Cross-domain empirical risk minimization for unbiased long-tailed classification," in *Proceedings of the AAAI Conference on Artificial Intelligence*, 2022.
- [21] H. Lee, S. Shin, and H. Kim, "Abc: Auxiliary balanced classifier for class-imbalanced semi-supervised learning," *Advances in Neural Information Processing Systems*, vol. 34, pp. 7082–7094, 2021.
- [22] Z. Lai, C. Wang, H. Gunawan, S. S. Cheung, and C. Chuah, "Smoothed adaptive weighting for imbalanced semi-supervised learning: Improve reliability against unknown distribution data," in *International Conference on Machine Learning*, 2022, pp. 11 828–11 843.
- [23] T. Wei, Q.-Y. Liu, J.-X. Shi, W.-W. Tu, and L.-Z. Guo, "Transfer and share: Semi-supervised learning from long-tailed data," *Machine Learning*, 2022.
- [24] J. Kim, Y. Hur, S. Park, E. Yang, S. J. Hwang, and J. Shin, "Distribution aligning refinery of pseudo-label for imbalanced semi-supervised learning," *Advances in Neural Information Processing Systems*, vol. 33, pp. 14 567–14 579, 2020.
- [25] C. Wei, K. Sohn, C. Mellina, A. Yuille, and F. Yang, "Crest: A class-rebalancing self-training framework for imbalanced semi-supervised learning," in *Proceedings of the IEEE/CVF Conference on Computer Vision and Pattern Recognition*, 2021, pp. 10 857–10 866.
- [26] B. Ye, K. Gan, T. Wei, and M.-L. Zhang, "Bridging the gap: Learning pace synchronization for open-world semi-supervised learning," *arXiv preprint arXiv:2309.11930*, 2023.
- [27] Y. Oh, D.-J. Kim, and I. S. Kweon, "Daso: Distribution-aware semantics-oriented pseudo-label for imbalanced semi-supervised learning," in *Proceedings of the IEEE/CVF Conference on Computer Vision and Pattern Recognition*, 2022, pp. 9786–9796.
- [28] T. Wei and K. Gan, "Towards realistic long-tailed semi-supervised learning: Consistency is all you need," in *Proceedings of the IEEE/CVF Conference on Computer Vision and Pattern Recognition*, 2023, pp. 3469–3478.
- [29] C. Du, Y. Han, and G. Huang, "Simpro: A simple probabilistic framework towards realistic long-tailed semi-supervised learning," *arXiv preprint arXiv:2402.13505*, 2024.
- [30] Y. Zhang, B. Hooi, L. Hong, and J. Feng, "Self-supervised aggregation of diverse experts for test-agnostic long-tailed recognition," *Advances in Neural Information Processing Systems*, vol. 35, pp. 34 077–34 090, 2022.
- [31] A. K. Menon, S. Jayasumana, A. S. Rawat, H. Jain, A. Veit, and S. Kumar, "Long-tail learning via logit adjustment," in *International Conference on Learning Representations*, 2020.
- [32] B. Kang, S. Xie, M. Rohrbach, Z. Yan, A. Gordo, J. Feng, and Y. Kalantidis, "Decoupling representation and classifier for long-tailed recognition," in *International Conference on Learning Representations*, 2020.
- [33] Z. Zhong, J. Cui, S. Liu, and J. Jia, "Improving calibration for long-tailed recognition," in *Proceedings of the IEEE/CVF conference on computer vision and pattern recognition*, 2021, pp. 16 489–16 498.
- [34] J. Ren, C. Yu, X. Ma, H. Zhao, S. Yi *et al.*, "Balanced meta-softmax for long-tailed visual recognition," *Advances in Neural Information Processing Systems*, vol. 33, pp. 4175–4186, 2020.
- [35] D. Berthelot, N. Carlini, E. D. Cubuk, A. Kurakin, K. Sohn, H. Zhang, and C. Raffel, "Remixmatch: Semi-supervised learning with distribution matching and augmentation anchoring," in *International Conference on Learning Representations*, 2019.
- [36] Y. Fan, D. Dai, A. Kukleva, and B. Schiele, "Coss: Co-learning of representation and classifier for imbalanced semi-supervised learning," in *Proceedings of the IEEE/CVF Conference on Computer Vision and Pattern Recognition*, 2022, pp. 14 574–14 584.
- [37] H. Zhang, M. Cissé, Y. N. Dauphin, and D. Lopez-Paz, "mixup: Beyond empirical risk minimization," in *International Conference on Learning Representations*, 2018.
- [38] T. DeVries and G. W. Taylor, "Improved regularization of convolutional neural networks with cutout," *arXiv preprint arXiv:1708.04552*, 2017.
- [39] E. D. Cubuk, B. Zoph, J. Shlens, and Q. V. Le, "Randaugment: Practical automated data augmentation with a reduced search space," in *Proceedings of the IEEE/CVF conference on computer vision and pattern recognition workshops*, 2020, pp. 702–703.
- [40] E. Arazo, D. Ortego, P. Albert, N. E. O'Connor, and K. McGuinness, "Pseudo-labeling and confirmation bias in deep semi-supervised learning," in *IJCNN*, 2020, pp. 1–8.
- [41] X. Wang, J. Gao, M. Long, and J. Wang, "Self-tuning for data-efficient deep learning," in *ICML*, 2021, pp. 10 738–10 748.
- [42] Z. Huang, L. Shen, J. Yu, B. Han, and T. Liu, "Flatmatch: Bridging labeled data and unlabeled data with cross-sharpness for semi-supervised learning," *Advances in Neural Information Processing Systems*, vol. 36, pp. 18 474–18 494, 2023.
- [43] Z. Huang, X. Yu, D. Zhu, and M. C. Hughes, "Interlude: Interactions between labeled and unlabeled data to enhance semi-supervised learning," *arXiv preprint arXiv:2403.10658*, 2024.

- [44] A. Krizhevsky, G. Hinton *et al.*, "Learning multiple layers of features from tiny images," 2009.
- [45] A. Coates, A. Ng, and H. Lee, "An analysis of single-layer networks in unsupervised feature learning," in *Proceedings of the fourteenth international conference on artificial intelligence and statistics. JMLR Workshop and Conference Proceedings*, 2011, pp. 215–223.
- [46] A. Oliver, A. Odena, C. A. Raffel, E. D. Cubuk, and I. Goodfellow, "Realistic evaluation of deep semi-supervised learning algorithms," *Advances in neural information processing systems*, vol. 31, 2018.
- [47] S. Zagoruyko and N. Komodakis, "Wide residual networks," *arXiv preprint arXiv:1605.07146*, 2016.
- [48] I. Sutskever, J. Martens, G. Dahl, and G. Hinton, "On the importance of initialization and momentum in deep learning," in *International conference on machine learning*. PMLR, 2013, pp. 1139–1147.
- [49] B. T. Polyak, "Some methods of speeding up the convergence of iteration methods," *Ussr computational mathematics and mathematical physics*, vol. 4, no. 5, pp. 1–17, 1964.
- [50] Y. Nesterov, "A method of solving a convex programming problem with convergence rate $o(1/k^2)$," in *Sov. Math. Dokl.*, vol. 27.
- [51] I. Loshchilov and F. Hutter, "Sgdr: Stochastic gradient descent with warm restarts," *arXiv preprint arXiv:1608.03983*, 2016.
- [52] M. Huh, P. Agrawal, and A. A. Efros, "What makes imagenet good for transfer learning?" *arXiv preprint arXiv:1608.08614*, 2016.
- [53] J. Deng, W. Dong, R. Socher, L.-J. Li, K. Li, and L. Fei-Fei, "Imagenet: A large-scale hierarchical image database," in *2009 IEEE conference on computer vision and pattern recognition*. Ieee, 2009, pp. 248–255.
- [54] M. Jia, L. Tang, B.-C. Chen, C. Cardie, S. Belongie, B. Hariharan, and S.-N. Lim, "Visual prompt tuning," in *European Conference on Computer Vision*. Springer, 2022, pp. 709–727.
- [55] S. Chen, C. Ge, Z. Tong, J. Wang, Y. Song, J. Wang, and P. Luo, "Adaptformer: Adapting vision transformers for scalable visual recognition," *NeurIPS*, vol. 35, pp. 16 664–16 678, 2022.
- [56] T. Wei, J.-X. Shi, W.-W. Tu, and Y.-F. Li, "Robust long-tailed learning under label noise," *arXiv preprint arXiv:2108.11569*, 2021.
- [57] L. Van der Maaten and G. Hinton, "Visualizing data using t-sne," *Journal of Machine Learning Research*, vol. 9, no. 11, 2008.
- [58] A. Radford, J. W. Kim, C. Hallacy, A. Ramesh, G. Goh, S. Agarwal, G. Sastry, A. Askell, P. Mishkin, J. Clark *et al.*, "Learning transferable visual models from natural language supervision," in *ICML*, 2021, pp. 8748–8763.
- [59] H. Liu, D. Tam, M. Muqeeth, J. Mohta, T. Huang, M. Bansal, and C. A. Raffel, "Few-shot parameter-efficient fine-tuning is better and cheaper than in-context learning," *NeurIPS*, vol. 35, pp. 1950–1965, 2022.
- [60] J.-X. Shi, T. Wei, Z. Zhou, X.-Y. Han, J.-J. Shao, and Y.-F. Li, "Parameter-efficient long-tailed recognition," *arXiv preprint*, 2023.
- [61] Z. Yang, M. Ding, Y. Guo, Q. Lv, and J. Tang, "Parameter-efficient tuning makes a good classification head," *arXiv preprint*, 2022.
- [62] K. Gan and T. Wei, "Erasing the bias: Fine-tuning foundation models for semi-supervised learning," *arXiv preprint arXiv:2405.11756*, 2024.
- [63] A. Dosovitskiy, L. Beyer, A. Kolesnikov, D. Weissenborn, X. Zhai, T. Unterthiner, M. Dehghani, M. Minderer, G. Heigold, S. Gelly *et al.*, "An image is worth 16x16 words: Transformers for image recognition at scale," *arXiv preprint*, 2020.
- [64] G. Chen, F. Liu, Z. Meng, and S. Liang, "Revisiting parameter-efficient tuning: Are we really there yet?" *arXiv preprint*, 2022.
- [65] E. J. Hu, Y. Shen, P. Wallis, Z. Allen-Zhu, Y. Li, S. Wang, L. Wang, and W. Chen, "Lora: Low-rank adaptation of large language models," *arXiv preprint*, 2021.